Jia et al. Stem Cell Research & Therapy (2025) 16:119
https://doi.org/10.1186/s13287-025-04258-w

Stem Cell Research & Therapy

RESEARCH Open Access

The local pulsatile parathyroid hormone delivery system induces the osteogenic differentiation of dental pulp mesenchymal stem cells to reconstruct mandibular defects

Yuanyuan Jia[1†], Mianmian Duan[1†], Yan Yang[2], Duchenhui Li[1], Dongxiang Wang[1] and Zhenglong Tang[1*]

Abstract

Background Tumors and injuries often lead to large mandibular defects. Accelerating the osteogenesis of large bone defect areas is a major concern in current research. In this study, dental pulp mesenchymal stem cells (DPSCs) were used as seed cells, and the local pulsatile parathyroid hormone (PTH) delivery system was used as an osteogenic-inducing active ingredient to act on DPSCs and osteoblasts, which were applied to the jaw defect area to evaluate its therapeutic effect on bone regeneration.

Methods Pulsatile delivery systems, both with and without PTH, were developed following the protocols outlined in our previous study. In vitro, the biocompatibility of the pulsatile delivery system with DPSCs was assessed using the Cell Counting Kit-8 (CCK8) assay and live/dead cell staining. Osteogenic differentiation was evaluated through alkaline phosphatase staining and alizarin red staining. In vivo, critical bone defects with a diameter of 10 mm were created in the mandibles of white rabbits. The osteogenic effect was further assessed through gross observation, X-ray imaging, and histological examination.

Results In vitro experiments using CCK8 assays and live/dead cell staining demonstrated that DPSCs successfully adhered to the surface of the PTH pulsatile delivery system, showing no significant difference compared to the control group. Furthermore, alkaline phosphatase staining and Alizarin Red staining confirmed that the localized pulsatile parathyroid hormone delivery system effectively induced the differentiation of DPSCs into osteoblasts, leading to the secretion of abundant calcium nodules. Animal studies further revealed that the PTH pulsatile delivery system promoted the osteogenic differentiation of DPSCs, facilitating the repair of critical mandibular bone defects.

†Yuanyuan Jia and Mianmian Duan contributed equally to this work.

Yuanyuan Jia and Mianmian Duan are co-first authors with equal contributions.

*Correspondence:
Zhenglong Tang
1985149363@qq.com

Full list of author information is available at the end of the article

Conclusion The rhythmic release of PTH from the pulsatile delivery system effectively induces the osteogenic differentiation of DPSCs. By leveraging the synergistic interaction between PTH and DPSCs, this approach facilitates the repair of extensive mandibular bone defects.

Introduction

Reconstruction of mandibular defects caused by tumors, trauma, or infections remains a significant clinical challenge due to the mandible's unique anatomical complexity and functional demands [1]. Various strategies have been developed to address this issue, including autologous bone grafting, allografts, and artificial implants. However, these approaches often face limitations such as inadequate bone availability, donor site morbidity, potential immune rejection, and restricted regenerative capacity at the defect site [2, 3]. In this context, stem cell-based regenerative therapies have emerged as a promising alternative for mandibular reconstruction, offering a source of osteogenic cells to promote bone formation and repair [4].

Mesenchymal stem cells (MSCs) have been extensively studied in bone tissue engineering due to their multilineage differentiation potential and immunomodulatory properties [5]. Among them, dental pulp-derived mesenchymal stem cells (DPSCs) and stem cells from human exfoliated deciduous teeth (SHEDs) have garnered significant attention for their potential in tissue formation as well as their robust paracrine signaling and immunomodulatory capabilities [6]. Notably, DPSCs are easily isolated and obtained from extracted or discarded teeth, providing an abundant and accessible cell source for regenerative medicine. This accessibility minimizes the risk of complications, offering distinct advantages over bone marrow and embryonic stem cells [7].

DPSCs, in particular, have demonstrated remarkable osteogenic differentiation potential both in vitro and in vivo. Furthermore, they secrete bioactive molecules that enhance the regenerative capacity of surrounding cells [8]. Numerous studies have indicated that DPSCs and SHEDs can facilitate healing and reconstruction in various jaw-related conditions, including tooth implantation [9], alveolar bone loss due to periodontitis [10], and fractures [11]. These compelling attributes position DPSCs as a highly promising candidate for mandibular tissue engineering.

Nevertheless, the precise mechanisms that regulate the osteogenic differentiation of DPSCs remain incompletely understood, highlighting the need for innovative strategies to boost their osteogenic potential in a targeted and efficient manner.

MSCs are regulated their growth and differentiation through hormones, growth factors, and mechanical stimulation [12–16]. Parathyroid hormone (PTH), a critical regulator of calcium and phosphate metabolism, has been shown to stimulate the proliferation and osteogenic differentiation of MSCs by activating intracellular signaling pathways associated with osteoblastogenesis [17, 18]. Beyond increasing the number of osteoblasts, PTH enhances bone remodeling and accelerates bone regeneration, making it an effective therapeutic tool for repairing bone defects. Traditionally, PTH is delivered systemically via subcutaneous injection [19–21]; however, this method results in low localized bioavailability and systemic side effects, limiting its application for treating localized bone defects, such as those found in the mandible [22, 23].

To overcome these limitations, significant attention has recently been directed toward developing advanced local delivery systems for PTH. These systems enable controlled or pulsed release of PTH directly at the defect site, ensuring sustained therapeutic efficacy while reducing off-target effects [24, 25]. In previous research, we successfully designed a pulsed-release PTH system with excellent mechanical properties and biocompatibility, which significantly improved mandibular fracture healing in a rat model [26]. Although these findings are promising, further investigation is required to determine whether this system can induce the osteogenic differentiation of DPSCs and facilitate the repair of mandibular defects.

In this study, we explored an innovative, locally applied PTH delivery system combined with DPSCs to promote bone regeneration in mandibular defects. Our hypothesis posited that the pulsed release of PTH would not only enhance the osteogenic differentiation of DPSCs but also stimulate the osteogenic activity of adjacent osteoblasts, creating a synergistic effect to improve bone repair. This research offers valuable insights into the application of locally engineered biological systems for tissue engineering and paves the way for the development of more effective strategies for mandibular reconstruction (Fig. 1).

Materials and methods

Collection and characterization of human dental pulp-derived mesenchymal stem cells (hDPSCs)

Isolation, culture and identification

Permanent teeth and third molars, free from lesions and caries, were extracted for orthodontic purposes at the Oral and Maxillofacial Surgery Clinic of the Stomatological Hospital, Guizhou Medical University. These specimens were obtained from healthy individuals aged 12 to 30 years. DPSCs were isolated following the Gronthos protocol [27], with modifications applied by our

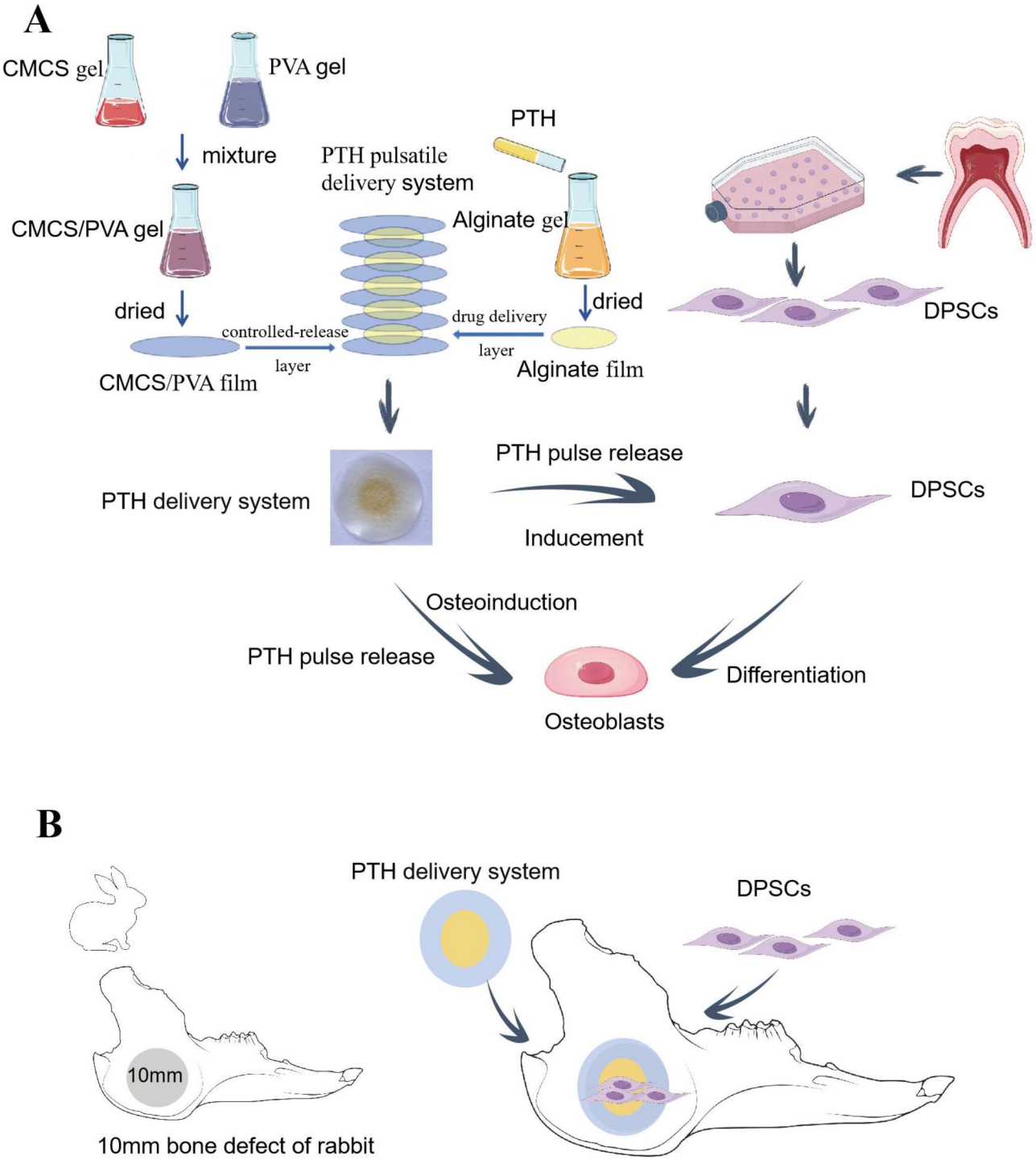

Fig. 1 **(A)** A schematic illustration depicting the process of extracting DPSCs and preparing the PTH pulsatile delivery system. **(B)** The synergistic effect of DPSCs combined with the PTH pulsatile delivery system on the bone defect area in the rabbit mandible

laboratory. The isolated cells were cultured in low-glucose DMEM, supplemented with 10% fetal calf serum and 1% penicillin-streptomycin, and incubated at 37 °C in a 5% CO_2 environment. The culture medium was refreshed every 2–3 days. When the cells reached approximately 80% confluence, they were passaged. Cells at passage 3 (P3) were selected for subsequent experiments. After 21 days of culture, flow cytometry analysis was performed on P3 cells to confirm the expression of MSC markers.

This study received approval from the Ethics Committee of the School of Stomatology at Guizhou Medical

University (Approval No. 1, 2022). Informed consent was duly obtained from all participating volunteers.

Multilineage differentiation in vitro

The cells were cultured in 6-well plates using an osteogenic induction medium composed of 50 mg/mL ascorbic acid, 10 mM β-glycerophosphate, and 10 nM dexamethasone (all purchased from Sigma-Aldrich), supplemented with 10% FBS, for a period of 21 days. Following the culture period, the cells were rinsed twice with PBS and fixed with 4% polyoxymethylene (Sigma-Aldrich, USA) for 15 min. Subsequently, the cells were stained using Alizarin Red S (Sigma-Aldrich, USA).

For adipogenic induction, the cells were cultured for 21 days in an adipogenic induction medium comprising 1 mM IBMX, 0.4 mM indomethacin, 0.2 μM dexamethasone, 0.02 mg/mL insulin, 100 μg/mL streptomycin, 100 U/mL penicillin, 10% FBS, and α-MEM. The cultures were then stained with 0.3% (w/v) Oil Red O (Sigma-Aldrich) prepared in 60% isopropanol for 60 min.

For chondrogenic induction, DMEM supplemented with 1X ITS, 1 mM sodium pyruvate, 100 nM dexamethasone, 50 μg/mL ascorbate-2-phosphate, 40 μg/mL L-proline, and 10 ng/mL TGF-β3 (Sigma-Aldrich Corp., St. Louis, MO, USA) was utilized. The cells were cultured for 28 days at 37 °C in a 5% CO_2 incubator, with the medium replaced every 2–3 days to maintain optimal conditions [28]. To analyze chondrogenic lineage differentiation, the cells were fixed using 4% paraformaldehyde and stained for mucopolysaccharides with 0.1% toluidine blue (TB).

Flow cytometric

DPSCs (2×10^5 cells) were subjected to trypsinization, then harvested. The cells (1×10^6/100 μL) were resuspended and incubated with fluorescein isothiocyanate (FITC)-conjugated anti-human monoclonal antibodies against CD34, CD45, CD90, and CD104 (1:100 dilution; BD Biosciences, San Jose, CA, USA) in PBS supplemented with 3% FBS. The incubation was conducted for 1 h in the dark at room temperature. Finally, the samples were analyzed using a flow cytometer (FACS Calibur; BD Biosciences, Franklin Lakes, NJ, USA) with CellQuest PRO™ software (BD Biosciences).

Preparation of the PTH pulsatile delivery system

Based on a prior study [26], a long-term pulsed release system incorporating PTH (PTH pulsatile delivery system) and a counterpart without PTH (blank delivery system) were developed. Both systems demonstrated excellent biocompatibility and non-toxicity.

DPSC cytotoxicity evaluation of the system

The pulsatile delivery system was immersed in a complete medium. To evaluate system degradation, extract solutions were collected after the system had been soaked for four weeks. Simultaneously, 5,000 DPSCs were seeded per well and cultured in 96-well plates under varying immersion durations. In a separate experiment, DPSCs were treated with 20 μL of Cell Counting Kit-8 (CCK-8) reagent (GlpBio, USA) and incubated at 37 °C for 1, 3, 5, or 7 days. Absorbance measurements at 450 nm were then taken using a microplate reader (Molecular Devices, USA).

The biosafety of the pulsatile delivery system for DPSCs was assessed through live/dead cell staining. The delivery platform consisted of a 60 mm diameter Petri dish, with DPSCs seeded at a density of 2×10^4 cells/mL. After a 24-hour incubation period to allow for cell adhesion, the non-adherent cells were rinsed away using PBS buffer. The remaining cells were then stained with a live/dead cell staining kit (Meilun Bio, China) and visualized under a fluorescence microscope (Olympus Corporation, Tokyo, Japan).

Osteogenic differentiation experiments

The cells were categorized into four groups: Group A (CTRL), treated with the complete medium; Group B (OIM), treated with the osteogenic induction medium; Group C (blank system), incorporating the blank system and the complete medium; and Group D (PTH system), consisting of the PTH delivery system combined with the complete medium. Following 7 and 14 days of culture, the medium was removed, and 4% paraformaldehyde was added to the cells. The cells were then fixed at 4 °C in the dark. To assess the early osteogenic differentiation performance of the PTH pulsatile delivery system on DPSCs, alkaline phosphatase (ALP) staining was performed using an ALP kit. After 21 and 28 days of osteogenic induction, the samples were similarly fixed with 4% paraformaldehyde at 4 °C in the dark. At this stage, an Alizarin Red S staining kit was employed to evaluate the extent of osteogenic mineralization in the different groups.

In vivo PTH pulsatile delivery system assay

Animal model

The study adhered to the ARRIVE guidelines 2.0. All mature New Zealand White rabbits (weighing 2.5 ± 0.5 kg) were handled in compliance with the United States National Research Council's Guide for the Care and Use of Laboratory Animals and the ethical standards of the Guizhou Medical University Institutional Animal Care and Use Committee (Approval Number: Protocol 2001340). The rabbits were housed in a Specific Pathogen-Free (SPF) environment at the Animal Experimentation Center of Guizhou Medical University.

A total of 72 adult rabbits were randomly selected and housed individually in ventilated cages (IVCs). They were maintained under a 12-hour light/dark cycle at a controlled temperature of 22 ± 2 °C with a humidity level of 50 ± 10%. Throughout the study, the rabbits were allowed free movement within their cages and provided ad libitum access to food and water. Prior to the initiation of experimental procedures, all animals underwent a seven-day acclimation period.

The rabbits were randomly divided into six groups as follows: (1) Defect–the mandibular defect was left untreated; (2) Blank system–the defect was covered with a blank delivery system; (3) DPSC–the defect was filled with a DPSC suspension containing 1×10^7 cells/mL; (4) PTH system–the defect was covered with a PTH delivery system; (5) DPSC + blank system–the defect was filled with a DPSC suspension containing 1×10^7 cells/mL and covered with a blank delivery system; and (6) DPSC + PTH system–the defect was filled with a DPSC suspension containing 1×10^7 cells/mL and covered with a PTH delivery system.

Surgical procedure

During surgery, the animals were anesthetized through an intramuscular (IM) injection combining ketamine (35 mg/kg) and 2% xylazine hydrochloride (2 mg/kg). Once the animals were fully unconscious, a trichotomy was performed, and the mandibular angular skin of each animal was treated with 10% povidone-iodine for asepsis. The surgical area was carefully isolated to maintain sterility. A single 2.5 cm incision was then made along the inferior margin of the mandible. The soft tissue was gently separated to expose the bone surface. In each rabbit, 10-mm circular penetrating defects were created in the parietal bone using a trephine bur attached to a low-speed handpiece. This process was conducted under continuous irrigation with 0.9% sterile saline to minimize tissue damage and maintain a clean surgical field.

Macroscopic observation

To assess the extent of defect healing, the rabbits were humanely euthanized with a pentobarbital sodium and phenytoin overdose (3 ml IV; Euthasol®, 390 mg pentobarbital sodium, 50 mg phenytoin sodium/ml, Virbac AH, Inc. Fort Worth, TX) at 14 and 28 days post-surgery.

Images of the rabbit mandibular bone defect areas were then captured. Macroscopic observations were performed by an independent observer who was blinded to the treatment groups.

Imaging evaluation

The radiodensity of the mandibular defect area across different groups was evaluated, and the extent of new bone formation within the defect site was analyzed. Digital X-rays were captured using a Heliodent Plus D3507 device (Germany) under standardized conditions (60 kV, 7 mA, 0.03 s). To ensure parallel radiation between the X-ray sensor and the jawbone, the sensor's position was meticulously adjusted to align with the morphology of the mandibular defect area. The critical size defect's measurement region, referred to as the region of interest (ROI), was used to assess radioopacity. The corresponding radiographic data were then quantified using ImageJ software.

Histological and immunohistochemical assessment

All samples were fixed in 10% paraformaldehyde, dehydrated through a graded ethanol series, embedded in paraffin, and sectioned to a thickness of 6 μm using standard histological procedures. The sections were then stained with hematoxylin-eosin (H&E) (Nanjing Jiancheng Bioengineering, China) and Masson trichrome staining (Leagene Biotechnology, China). For immunohistochemistry, deparaffinized and rehydrated sections were incubated overnight at 4 °C with primary antibodies targeting Runx2 (1:300, Servicebio), OCN (1:200, Servicebio), or OPN (1:1000, Servicebio), followed by incubation with the appropriate secondary antibodies. Immunostaining was performed using the Vectastain ABC kit and Nova-RED peroxidase substrate kit (Vector Labs, Burlingame, CA, USA). Sections from the repair site were analyzed for internal optical density (IOD) using Image-Pro Plus 6.0 software.

Statistical analysis

Statistical analyses were conducted using SPSS version 26.0. All data exhibited a normal distribution with homogeneous variance, and the analyses were performed using a one-way independent analysis of variance (ANOVA). A p-value of less than 0.05 was considered the threshold for statistical significance.

Results

Culture and characterization of hDPSCs

Fibroblast-like clonal cells were successfully derived from dental pulp tissue through limiting dilution and colony cloning (Supplementary Figure S1). The evaluation of their morphology, colony-forming capacity, immunophenotypic profile, and multipotent differentiation potential confirmed the successful isolation of mesenchymal stem cells.

Effects of the pulsatile delivery system on the proliferation and activity of DPSCs

The outcomes of the CCK-8 assay, which evaluated the impact of the pulsatile delivery system on DPSC proliferation, are presented in Fig. 2A. No statistically significant differences in OD values were observed between the

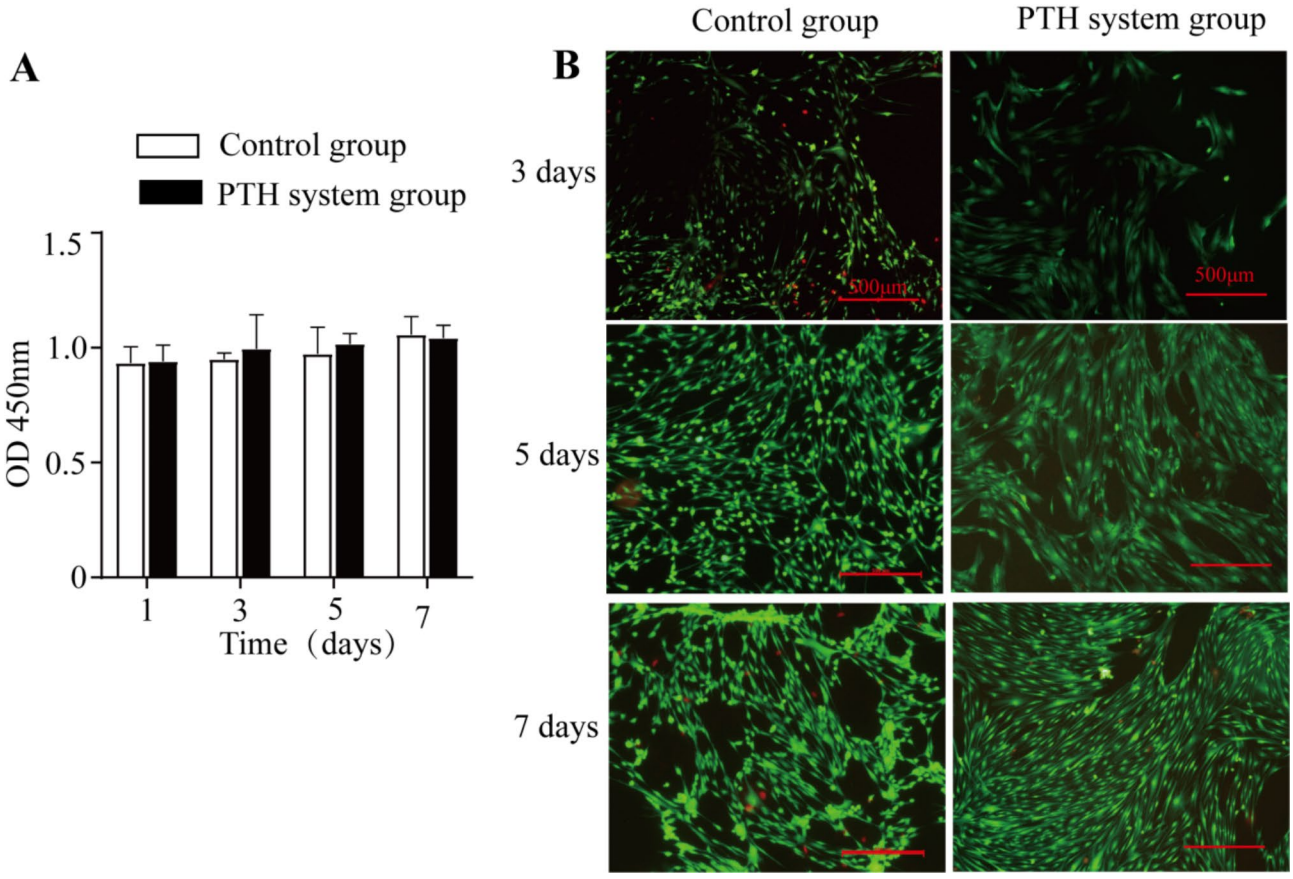

Fig. 2 Impact of the pulsed sustained release system on the proliferation and activity of DPSCs. **(A)** Assessment of DPSC viability determined using the CCK-8 assay ($n=6$). **(B)** Live/dead cell staining following the coculture of DPSCs with the PTH system. Scale bar: 500 μm

control and experimental groups on days 1, 3, 5, and 7 ($p>0.05$, Fig. 2A).

The viability of DPSCs within type I and type II collagen hydrogels was evaluated using a LIVE/DEAD® cell viability assay kit. After six days of culture, the majority of the cells in the hydrogels were viable, as shown in Fig. 2B. The cells displayed an elongated morphology with multiple processes extending within the hydrogels. Quantitative analysis of live and dead cells demonstrated that the percentage of viable DPSCs exceeded 95% across all groups (Fig. 2B). Moreover, no significant differences were observed between the groups.

PTH delivery system enhances DPSC osteogenic differentiation capacity

ALP activity was obtained after the DPSCs were cultured for 7 days in the OIM group and PTH system group. Furthermore, ALP activity was greater after 14 days (Fig. 3A-H). The resultant of p-nitrophenol phosphate was assayed using an enzymatic activity assay (Nanjing Jiancheng, China) at 520 nm (Fig. 3Q). On day 21, extensive positive ARS staining was observed in the OIM group and the PTH system group. Similarly, calcium deposition levels on day 28 were higher in the OCM group compared to the control group (Fig. 3I-P). To quantify this, the orange dye was dissolved in 10 mM sodium phosphate and 10% cetylpyridinium chloride (Solarbio, China), and optical density (OD) was recorded at 550 nm using a microplate reader (Molecular Devices, USA) (Fig. 3Q). These findings demonstrate that the PTH system accelerates mineralization and promotes osteogenic differentiation of DPSCs. Throughout the observation period, both ALP and ARS staining remained negative in the CTRL group and the blank system group.

Macroscopic evaluation of mandibular bone defects

All the rabbits were in good health. All the surgical sites healed without complications.

Two weeks post-surgery, minimal new bone formation was observed in the defect group. In contrast, the neotissue in the other groups showed slight integration with the adjacent bone, though it was irregularly filled with soft tissue (Fig. 4A–F). By four weeks post-surgery, macroscopic evaluation of the full-thickness bone defect sites in the DPSC + PTH system group revealed smooth, glossy surfaces with completely filled defects, in

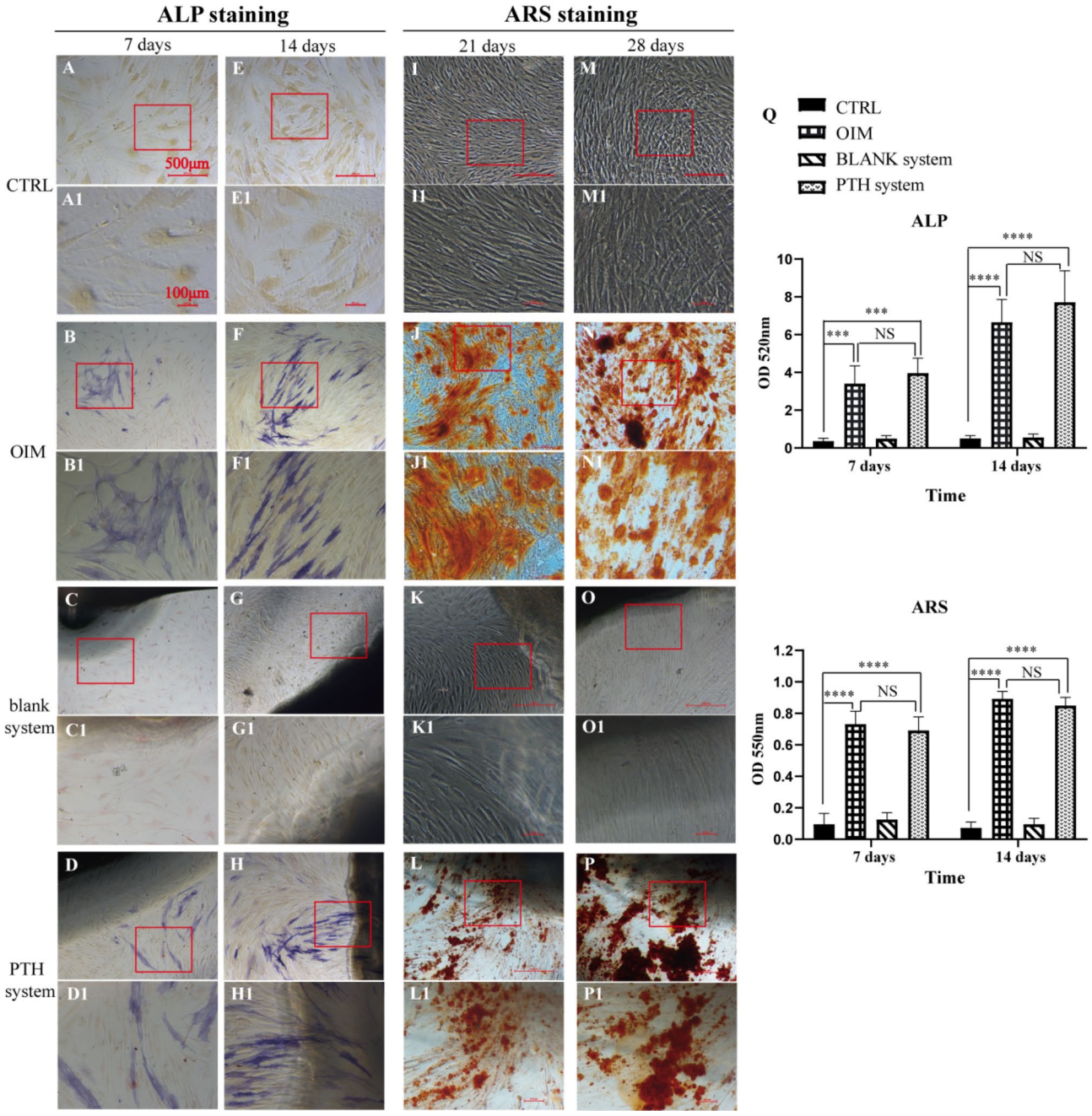

Fig. 3 ALP and ARS staining results following the coculture of the PTH delivery system with DPSCs. **(A-H)** ALP staining; **(I-P)** ARS staining. Experimental groups: CTRL, complete medium; OIM, osteogenic induction medium; blank system, blank system + complete medium; PTH system, PTH delivery system + complete medium. Red boxes highlight the magnified areas. Scale bars: (A-P) 500 μm, (A1-P1) 100 μm. Statistical significance: ***$p < 0.001$, ****$p < 0.0001$

stark comparison to the outcomes observed in the other groups (Fig. 4M–R).

Radiographs revealed radiolucent bone defects in the mandibles of the experimental groups. By the 2-week mark, the PTH system group and the DPSC + PTH system group exhibited increased radiopacity in critical bone defects due to their heightened radiographic density, which was notably higher than that observed in the other groups (Fig. 4G-L). A significant increase ($p < 0.0001$) in radiographic density was identified in both the PTH system group and the DPSC + PTH system group when compared to the defect group (Fig. 4Y). At 4 weeks, the intervention groups demonstrated a markedly higher radiopacity than the control group (Fig. 4S-X), with the DPSC + PTH system group achieving the highest imaging density among all groups (Fig. 4Y).

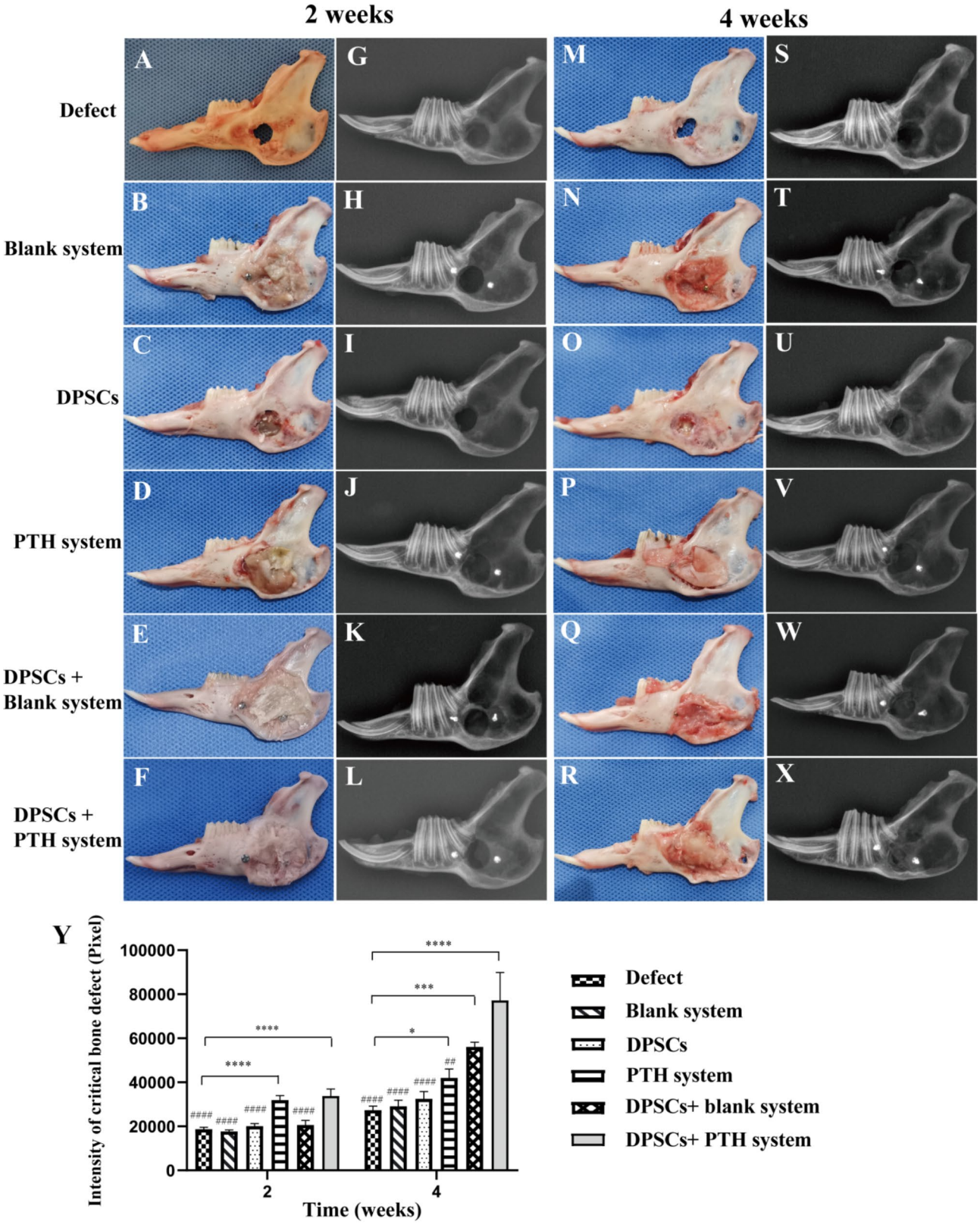

Fig. 4 Gross morphology and X-ray images of each group. **(A-L)** 2 weeks post-surgery. **(M-X)** 4 weeks post-surgery. **(Y)** Grayscale X-ray values. Defect: mandibular defect; blank system: blank delivery system; DPSC: dental pulp stem cell + PTH delivery system; DPSC + blank system: dental pulp stem cell + blank delivery system; DPSC + PTH system: dental pulp stem cell + PTH delivery system. Statistical significance: *$p < 0.05$, ***$p < 0.001$, ****$p < 0.0001$, versus defect group; ##$p < 0.01$, ####$p < 0.0001$, versus DPSCs + PTH system group

H&E and Masson's trichrome staining results

H&E and Masson's trichrome staining confirmed the formation of new bone. As illustrated in the H&E staining images (Fig. 5), no significant inflammatory reaction or necrosis was detected in any of the groups. In the defect group, fibrous connective tissue was absent in the center of the defect, while new bone formation and some chondrocytes were observed on either side of the defect. In contrast, fibrous connective tissue was evident in the defect area across the blank system group, DPSC group, and DPSC + blank system group. Additionally, new bone formation was observed adjacent to the fibrous connective tissue near the original bone tissue in these groups, with a more pronounced quantity of new bone identified in the DPSC and DPSC + blank system groups compared to the blank system group. In the PTH system group, scattered fibrous tissue was visible within the newly formed bone. Notably, the DPSC + PTH system group demonstrated a significant amount of mature bone tissue within the defect area, with this mature bone seamlessly integrated with the surrounding original bone.

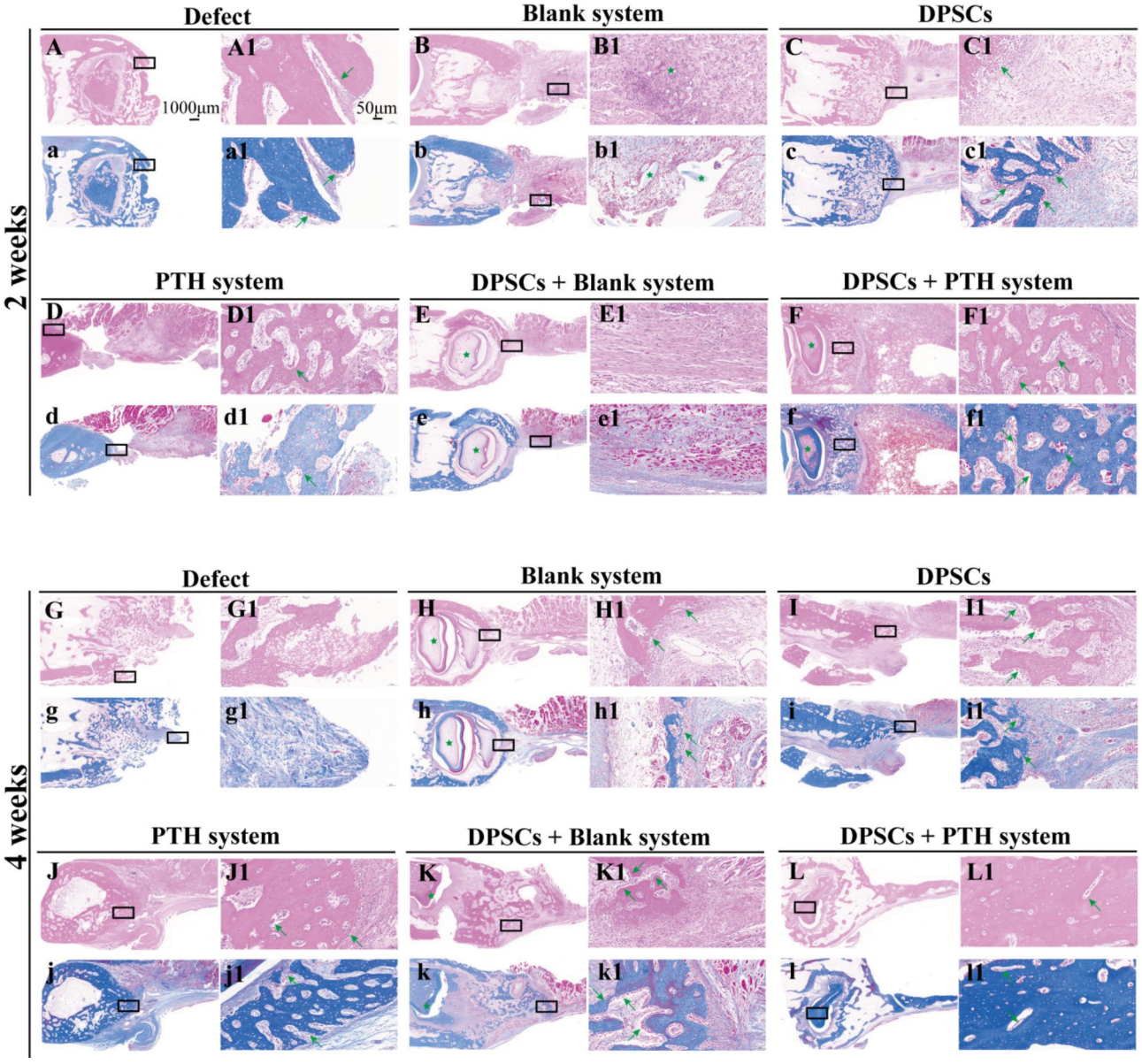

Fig. 5 H&E and Masson's trichrome staining conducted at 2 and 4 weeks post-bone regeneration. **(A-F)** 2 weeks post-surgery. **(G-L)** 4 weeks post-surgery. **(A-L)** H&E staining; **(a-l)** Masson trichrome staining. Defect: mandibular defect; blank system: blank delivery system; DPSC: dental pulp stem cell + PTH delivery system; DPSC + blank system: dental pulp stem cell + blank delivery system; DPSC + PTH system: dental pulp stem cell + PTH delivery system. The black boxes indicate enlarged areas, the green arrows indicate osteoblasts, and the green stars indicate system fragments. Scale bars: (A-L and a-l) 1000 μm, (A1-L1 and a1 - l1): 10 μm

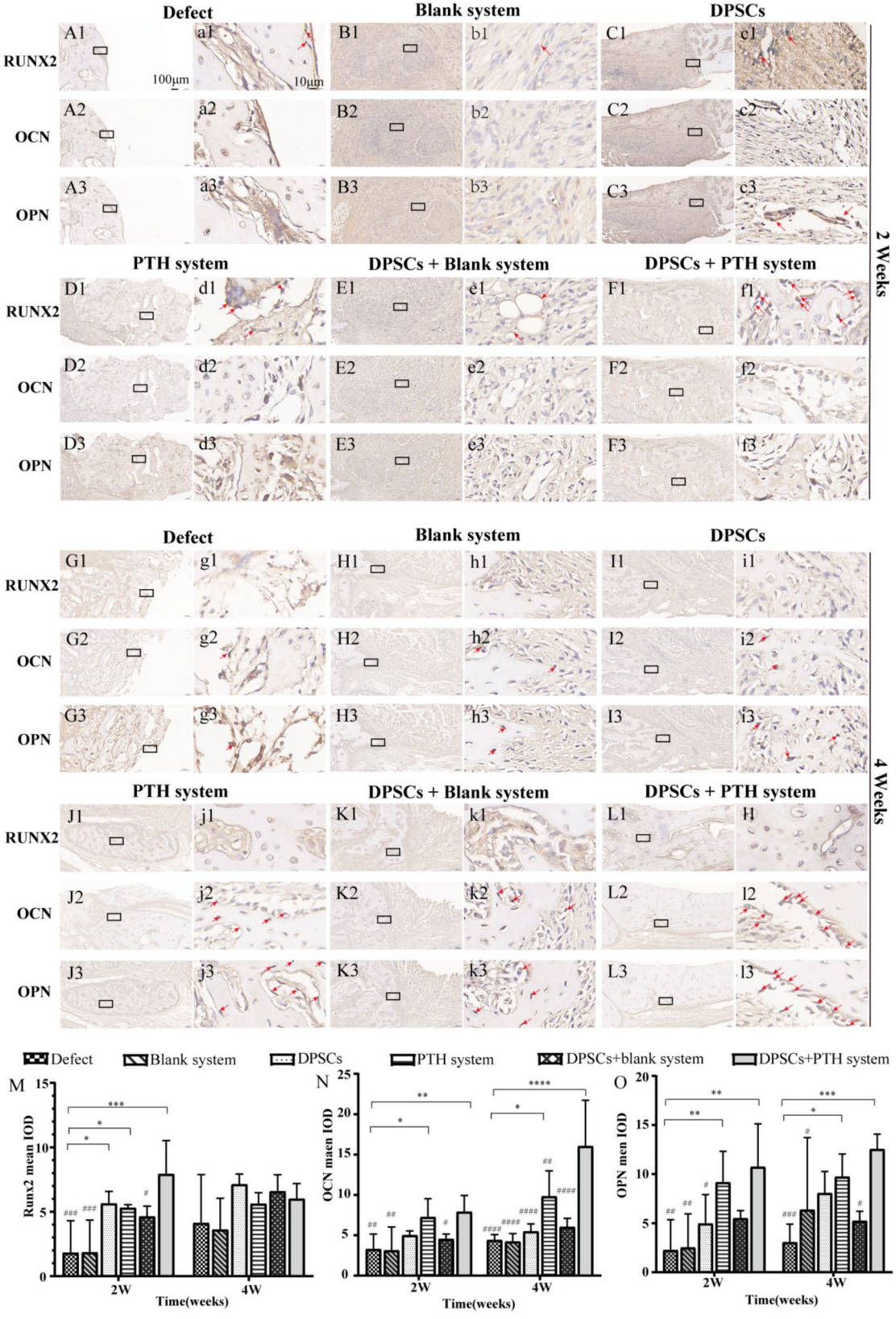

Fig. 6 (See legend on next page.)

(See figure on previous page.)

Fig. 6 Immunohistochemical staining results for Runx2, OCN, and OPN and semiquantitative scoring. **(A-F)** Immunohistochemistry 2 weeks post-surgery. **(G-L)** Immunohistochemistry 4 weeks post-surgery. **(M-O)** Semiquantitative analysis of immunohistochemistry (IOD) values. Defects: mandibular defect; blank system: blank delivery system; DPSC: dental pulp stem cell; PTH system: PTH delivery system; DPSC + blank system: dental pulp stem cell + blank delivery system; DPSC + PTH system: dental pulp stem cell + PTH delivery system. The black boxes indicate enlarged areas, and the red arrows indicate positive staining. Scale bars, (A-L) 100 μm and (a - l): 10 μm. Statistical significance: *$p < 0.05$, **$p < 0.01$, ***$p < 0.001$,****$p < 0.0001$, versus defect group; #$p < 0.05$, ##$p < 0.01$, ###$p < 0.001$, ####$p < 0.0001$, versus DPSCs + PTH system group

Masson's trichrome staining revealed that the defect remained evident in the center, with no formation of new tissue connections in the defect group (Fig. 5). In the DPSC and DPSC + blank system groups, a greater accumulation of fibrous tissue was observed in the defect area compared to the blank system group, and new bone tissue was identified adjacent to the original bone tissue on both sides of the fibrous tissue. In the PTH system group, the defect area exhibited a substantial presence of fibrous connective tissue, accompanied by scattered areas of ossification within the fibrous tissue. Notably, in the DPSC + PTH system group, mature bone tissue connections were observed within the defect area.

Immunohistochemistry analysis for osteogenic growth factors

The results of Runx2 immunohistochemical staining (Fig. 6) indicated that the intensity and area of hyperstained Runx2 surrounding the osteoblast nuclei were noticeably reduced in both the PTH system group and the DPSC + PTH system group compared to the other groups. This suggests that the expression of Runx2 in these groups was lower than in the others. At the four-week mark, no significant differences were observed among the PTH system group, the DPSC + PTH system group, and the MD group ($P > 0.05$) (Fig. 6M).

The results of OCN and OPN immunohistochemical staining demonstrated that the positive staining observed in the new bone matrix, osteoblasts, and osteocytes was significantly stronger in both the PTH system group and the DPSC + PTH system group compared to the defect group, blank system group, DPSC group, and DPSC + blank system group. Moreover, the staining in the DPSC + PTH system group exhibited a deeper color and a broader area than that of the PTH system group (Fig. 6). The mean integrated optical density (IOD) values were comparable across the different groups, with the PTH system group and DPSC + PTH system group showing significantly higher IOD values than the defect group ($p < 0.01$) (Fig. 6N, O).

Discussion

DPSCs have gained increasing attention as a promising cell source for bone tissue engineering due to their accessibility, rapid proliferation, multilineage differentiation capacity, and immunomodulatory properties [29, 30]. Compared with bone marrow mesenchymal stem cells (BMSCs)—the most extensively used stem cells in bone regeneration research—DPSCs offer distinct advantages, including the lack of invasive isolation procedures, fewer ethical concerns, and higher osteogenic differentiation potential in the craniofacial region [7, 31, 32]. While BMSCs have been gold-standard seed cells for bone engineering [33], emerging evidence suggests that DPSCs exhibit higher mineralization efficiency and comparable osteogenic marker expression in vivo [7, 34]. In our study, xenogeneic DPSCs, isolated via the tissue block method, expressed mesenchymal stem cell markers CD90 and CD105, demonstrated multilineage differentiation potential, and met the basic requirements for osteogenic regeneration, highlighting their potential for large-scale application in mandibular regeneration. Moreover, it is noted that the DPSC + blank system showed good osteogenic potential at 4 weeks in vivo, while it did not show significant osteogenic potential in in vitro experiments. This difference can be attributed to the in vivo microenvironment, which provides additional osteogenic cues (e.g., growth factors, vascularization) absent in vitro [35, 36].

Limitations of current PTH administration and role of pulsatile delivery systems

PTH is well established as a regulator of calcium and phosphorus metabolism and a stimulant for the osteogenic differentiation of mesenchymal stem cells [37, 38]. However, its clinical application has predominantly relied on intermittent subcutaneous injections, which are associated with challenges such as poor targeting efficiency, systemic side effects such as hypercalcemia, and low bioavailability at the defect site [39, 40]. Furthermore, in vitro applications of PTH typically require daily supplementation to avoid concentration fluctuations, leading to resource wastage and operational inefficiencies [41]. To overcome these limitations, we implemented a locally applied long-term pulsatile release system. This approach ensures the controlled, low-dose release of PTH while successfully mitigating the aforementioned drawbacks.

The biocompatibility and safety of the PTH pulsatile delivery system were confirmed through CCK8 assays and live–dead cell staining of DPSCs cocultured with the system, which indicated no cytotoxicity and excellent compatibility with DPSC growth. Importantly, the PTH released from the delivery system retained its biological activity, as evidenced by its ability to induce osteogenic differentiation in DPSCs in vitro.The innovative

pulsed-release mechanism also allowed for improved temporal synchronization with cellular processes, enhancing the osteogenic potential of MSCs—a hypothesis supported by prior studies on pulsed PTH delivery in bone tissue [26].

Large bone defects and in vivo proof of concept

In this study, we addressed a critical knowledge gap by exploring the ability of DPSCs and the PTH pulsatile system to regenerate large, non-healing mandibular bone defects. The rabbit mandibular defect model used in our experiments overcame the challenge of spontaneous healing observed in smaller or partial-thickness defect models [30]. Four weeks postoperatively, the DPSC + PTH system group exhibited robust bone regeneration, as confirmed by imaging, histological analyses, and mechanical assessments. Specifically, newly formed bone in the defect area was comparable to surrounding tissue in hardness, density, and structural integrity.

A key innovation of this work is the demonstration that xenogeneic DPSCs, combined with PTH pulsatile delivery, can repair critical-sized mandibular defects—a significant advance over prior studies limited to autologous DPSCs + bone substitute in small defects [7, 42]. In vivo, the DPSC + PTH group achieved complete defect healing with histomorphometric parameters comparable to native bone. This outcome surpasses reported results using BMSCs or adipose-derived stem cells (ADSCs) in similar models, where incomplete ossification and fibrous tissue infiltration were frequently observed [43–45].

Mechanistically, PTH not only regulated systemic calcium-phosphorus homeostasis but also directly induced DPSC osteogenesis. Histological staining and biochemical analyses provided additional insights into the bone repair processes. Masson staining revealed a dense collagen matrix in the defect area, while increases in serum markers such as PINP and OCN confirmed enhanced bone-forming activity during repair (Supplementary Figure S2). ALP expression, an early indicator of osteoblast maturation, was significantly higher in the DPSC + PTH group than in controls. These findings collectively indicate that the synergistic action of PTH and DPSCs facilitates the repair of mandibular defects by inducing osteogenic differentiation, stimulating osteoblast activity, and accelerating collagen synthesis and mineralized matrix deposition [46–49].

Mechanistic insights and areas for further exploration

Despite these promising results, this study was limited in its investigation of the molecular mechanisms by which PTH promotes DPSC-mediated bone regeneration. Previous studies have suggested that PTH-induced osteogenic differentiation involves activation of the cAMP/PKA signaling pathway and the Wnt/β-catenin pathways, which regulate osteoblast differentiation and bone matrix deposition [50–52]. Further investigation into these pathways in future studies could significantly advance our understanding of the molecular processes underlying bone healing and uncover new strategies to enhance the therapeutic potential of PTH-mediated bone regeneration.

Furthermore, while this study confirmed the role of the PTH pulsatile system in promoting bone repair, the potential for integrating dual biomolecules—such as PTH paired with BMP-2 or VEGF—within a single delivery system merits further investigation. By simultaneously targeting angiogenesis and osteogenesis, such combinations hold promise for significantly enhancing both the quality and speed of bone regeneration [53–55].

Limitations of the study

Although these advancements, our study has certain limitations that merit discussion. The molecular mechanisms by which PTH promotes the osteogenic differentiation of DPSCs remain unclear. Although the rabbit mandibular defect model proved to be a valuable proof-of-concept, future research should assess the long-term efficacy and safety of this approach in larger animal models or clinical applications. Furthermore, the host immune response to xenogeneic DPSCs remains a critical area for further investigation.

Despite these limitations, this study represents the first successful demonstration of xenogeneic DPSCs in combination with a PTH pulsatile delivery system for large mandibular defect repair. The results not only confirm the superior osteogenic differentiation capacity of DPSCs in the presence of PTH but also provide a foundation for developing an allogeneic DPSC bank for future clinical applications. This may be particularly beneficial for patients unable to provide their own autologous DPSCs.

Conclusion

In conclusion, our findings underscore the synergistic effects of DPSCs and PTH delivery in promoting mandibular bone regeneration. The pulsatile PTH delivery system, characterized by its biocompatibility and controlled release properties, effectively stimulated the osteogenic differentiation of DPSCs, facilitating the repair of substantial mandibular defects. Future research will aim to refine the delivery system, delve deeper into the molecular mechanisms underpinning PTH-induced osteogenesis, and assess the clinical viability of this approach through large-scale trials.

Abbreviations

ALP	Alkaline phosphatase.
ARS	Alizarin red S.
CCK-8	Cell counting kit-8.
CMCS	Carboxymethyl chitosan.

DPSCs	Dental pulp stem cells.
IOD	Integral Optical Density.
MSCs	Mesenchymal stem cells.
MTB	Methyl thymol blue.
OPN	Osteopontin.
OCN	Osteocalcin.
PTH	Parathyroid hormone.
Runx2	Runt-related transcription factor 2.
BMSCs	Bone marrow mesenchymal stem cells.
ADSCs	Adipose-derived stem cells.

Supplementary Information

The online version contains supplementary material available at https://doi.org/10.1186/s13287-025-04258-w.

Supplementary Material 1

Supplementary Material 2

Acknowledgements
The authors thank the Guizhou Provincial Science and Technology Department Key Project, Qiankehe Fundamentals ZK [2023] Key 036. The authors declare that they have not use AI-generated work in this manuscript.

Author contributions
Designed the research studies: Zhenglong Tang. Conducted the experiments: Yuanyuan Jia, Mianmian Duan, Duchenhui Li, Dongxiang Wang. Acquired the data: Mianmian Duan, Yan Yang. Analyzed the data: Zhenglong Tang, Yuanyuan Jia, Yan Yang and Mianmian Duan. Wrote the manuscript: Yuanyuan Jia and Mianmian Duan. Manuscript revision: Zhenglong Tang. All the authors have read and approved the final submitted manuscript.

Funding
The work was supported by the Guizhou Provincial Science and Technology Department Key Project, Qiankehe Fundamentals ZK [2023] Key 036.

Availability of supporting data
Data availability is not applicable to this article as no new data were created or analyzed in this study.All data in this research study are available from the corresponding author upon reasonable request.

Declarations

Ethical approval and consent to participate
The animal research involved in this work was approved by Ethics Committee of Guizhou Medical University. Title of the approved project: Natural Science Foundation of Guizhou Province for "Basic study on local pulse release of parathyroid hormone to promote fracture healing". The initial Ethics approval (No2001340) was obtained on June 2, 2020. The care and use of animals were performed strictly following the regulations on the management of experimental animals. The research on human DPSCs samples involved in this work was approved by the Ethics Committee of School of Stomatology affiliated to Guizhou Medical University. Title of the approved project: Natural Science Foundation of Guizhou Province for "Basic study on local pulse release of parathyroid hormone to promote fracture healing". The initial Ethics approval (Batch number: 2022 Lun Review No. 1) was obtained on January 17, 2022.

Consent for publication
Not applicable.

Competing interests
The authors declare that they have no known competing financial interests or personal relationships that could have appeared to influence the work reported in this paper.

Author details
[1]Department of Oral and Maxillofacial Surgery, School and Hospital of Stomatology, Guizhou Medical University, Guiyang 550000, China
[2]Center for Tissue Engineering and Stem Cell Research, Guizhou Medical University, Guiyang 550000, China

Received: 7 January 2025 / Accepted: 27 February 2025
Published online: 06 March 2025

References

1. Schultz BD, Sosin M, Nam A, Mohan R, Zhang P, Khalifian S, et al. Classification of mandible defects and algorithm for microvascular reconstruction. Plast Reconstr Surg. 2015;135(4):743e–754e. https://doi.org/10.1097/PRS.0000000000001106
2. Maduni LW, George JD. Kariyawasam Majuwana Gamage Prasanna P. A novel classification of bone graft materials. J Biomed Mater Res B Appl Biomater. 2022;110(7).
3. Daoud S, Zoabi A, Kasem A, Totry A, Oren D, Redenski I et al. Computer-assisted evaluation confirms spontaneous healing of donor site one year following bone block harvesting from mandibular retromolar region: A cohort study. Diagnostics (Basel, Switzerland). 2024;14(5).
4. Torrecillas-Baena B, Pulido-Escribano V, Dorado G, Gálvez-Moreno M, Camacho-Cardenosa M. Casado-Díaz A. Clinical potential of mesenchymal stem Cell-Derived exosomes in bone regeneration. J Clin Med. 2023;12(13).
5. Sun HH, Chen B, Zhu QL, Kong H, Li QH, Gao LN, et al. Investigation of dental pulp stem cells isolated from discarded human teeth extracted due to aggressive periodontitis. Biomaterials. 2014;35(35):9459–72.
6. Tatullo M, Marrelli M, Shakesheff KM, White LJ. Dental pulp stem cells: function, isolation and applications in regenerative medicine. J Tissue Eng Regen Med. 2015;9(11):1205–16.
7. Lee YC, Chan YH, Hsieh SC, Lew WZ, Feng SW. Comparing the osteogenic potentials and bone regeneration capacities of bone marrow and dental pulp mesenchymal stem cells in a rabbit calvarial bone defect model. Int J Mol Sci. 2019;20(20).
8. Shi S, Robey PG, Gronthos S. Comparison of human dental pulp and bone marrow stromal stem cells by cDNA microarray analysis. Bone. 2001;29(6):532–9.
9. Lymperi S, Ligoudistianou C, Taraslia V, Kontakiotis E, Anastasiadou E. Dental stem cells and their applications in dental tissue engineering. Open Dentistry J. 2013;7(1):76–81.
10. Saskianti T, Nugraha AP, Prahasanti C, Ernawati DS, Tanimoto K, Riawan W, et al. Study of alveolar bone remodeling using deciduous tooth stem cells and hydroxyapatite by vascular endothelial growth factor enhancement and Inhibition of matrix Metalloproteinase-8 expression in vivo. Clin Cosmet Invest Dentistry. 2022;14(Print):1179–357.
11. Yamakawa D, Kawase-Koga Y, Fujii Y, Kanno Y, Sato M, Ohba S et al. Effects of helioxanthin derivative-treated human dental pulp stem cells on fracture healing. Int J Mol Sci. 2020;21(23).
12. Khan F, Tanaka M. Designing smart biomaterials for tissue engineering. Int J Mol Sci. 2017;19(1).
13. Huynh NPT, Brunger JM, Gloss CC, Moutos FT, Gersbach CA, Guilak F. Genetic engineering of mesenchymal stem cells for differential matrix deposition on 3D woven scaffolds. Tissue Eng Part A. 2018;24(19–20):1531–44.
14. Liu H, MacQueen LA, Usprech JF, Maleki H, Sider KL, Doyle MG, et al. Microdevice arrays with strain sensors for 3D mechanical stimulation and monitoring of engineered tissues. Biomaterials. 2018;172(Electronic):1878–5905.
15. Yang B, Wei K, Loebel C, Zhang K, Feng Q, Li R et al. Enhanced mechanosensing of cells in synthetic 3D matrix with controlled biophysical dynamics. Nat Commun. 2021;12(1).
16. Su N, Gao P-L, Wang K, Wang J-Y, Zhong Y, Luo Y. Fibrous scaffolds potentiate the paracrine function of mesenchymal stem cells: A new dimension in cell-material interaction. Biomaterials. 2017;141(Electronic):1878–5905.
17. Bhandi S, Alkahtani A, Reda R, Mashyakhy M, Boreak N, Maganur PC et al. Parathyroid hormone secretion and receptor expression determine the age-related degree of osteogenic differentiation in dental pulp stem cells. J Pers Med. 2021;11(5).
18. Wang Y, Huang L, Qin Z, Yuan H, Li B, Pan Y, et al. Parathyroid hormone ameliorates osteogenesis of human bone marrow mesenchymal stem cells against glucolipotoxicity through p38 MAPK signaling. IUBMB Life. 2020;73(1):213–22.
19. Tang Z-L, Zhang W-J, Wang D-X, Chen J-M, Ma H, Wu D-R. An experimental study addressing the promotion of mandibular defect repair through the

intermittent subcutaneous injection of parathyroid hormone. J Oral Maxillofac Surg. 2014;72(2):419–30.
20. Tang Z-L, Bai S, Zhu P-N, Li Y-D, Wang D-X, Cai Y. An examination of differences in the new bone formation promoted by different doses of Recombinant human parathyroid hormone during mandibular distraction osteogenesis. Plast Reconstr Surg. 2016;137(2):e347–54.
21. An N, Li Y, Tang ZL, Chen XY, Wang DX, Gao Q. Expression of osteoprotegerin and receptor activator of nuclear factor kappa-B ligand in mandibular Ramus osteotomy healing with administration of different doses of parathyroid hormone. 2018;(1002-0098 (Print)). https://doi.org/10.3760/cma.j.issn.1002-0098.2018.06.010
22. Ning Z, Tan B, Chen B, Lau DSA, Wong TM, Sun T et al. Precisely controlled delivery of abaloparatide through injectable hydrogel to promote bone regeneration. Macromol Biosci. 2019;19(6).
23. Kenneth GS, Maria Luisa JP, Andrew B, Mattias CK, Thierry L. T., Romosozumab or alendronate for fracture prevention in women with osteoporosis. N Engl J Med. 2017;377(15).
24. Long J, Wang Y, Lu M, Etxeberria AE, Zhou Y, Gu P, et al. Dual-Cross-Linked magnetic hydrogel with programmed release of parathyroid hormone promotes bone healing. ACS Appl Mater Interfaces. 2023;15(30):35815–31.
25. Wojda SJ, Marozas IA, Anseth KS, Yaszemski MJ, Donahue SW. Impact of release kinetics on efficacy of locally delivered parathyroid hormone for bone regeneration applications. Tissue Eng Part A. 2021;27(3–4):246–55.
26. Jia Y, Duan M, Yang Y, Wang D, Dong Q, Liao J, et al. The promoting effect of a local pulsatile parathyroid hormone delivery on healing of the mandibular fracture in rats. Tissue Eng Part A. 2023;29(3–4):69–79.
27. Gronthos S, Mankani M, Brahim J, Robey PG, Shi S. Postnatal human dental pulp stem cells (DPSCs) in vitro and in vivo. Proc Natl Acad Sci. 2000;97(25):13625-30.
28. Shankargouda P, Ahmed A, Bassam Z, Khalid JA, Fuad MA, Hamsa Jameel B et al. Dose-Dependent effects of melatonin on the viability, proliferation, and differentiation of dental pulp stem cells (DPSCs). J Personalized Med. 2022;12(10).
29. Lina MaríaA-S, Dabeiba Adriana G-R, Nelly SR, Luis Maria R-L, Constanza M-C. Platelet-rich fibrin (PRF) modified nano-hydroxyapatite/chitosan/gelatin/alginate scaffolds increase adhesion and viability of human dental pulp stem cells (DPSC) and osteoblasts derived from DPSC. Int J Biol Macromol. 2024;273(0).
30. J G C. AEL, Q Z Z. SHSPH. A D L. DPSC-Derived extracellular vesicles promote rat jawbone regeneration. J Dent Res. 2022;102(3).
31. Mattei V, Delle Monache S. Dental pulp stem cells (DPSCs) and tissue regeneration: mechanisms mediated by direct, Paracrine, or autocrine effects. Biomedicines. 2023;11(2).
32. Sebastian G, Hanluo L, Simin L, Qian W, Tina K, Sebastian H et al. Shared genetic and epigenetic mechanisms between the osteogenic differentiation of dental pulp stem cells and bone marrow stem cells. Biomed Res Int. 2021;2021(0).
33. Paolo B, Xu C, Paul SF, Jeremy JM, Pamela GR, Paul JS et al. The meaning, the sense and the significance: translating the science of mesenchymal stem cells into medicine. Nat Med. 2013;19(1).
34. Aghajani F, Hooshmand T, Khanmohammadi M, Khanjani S, Edalatkhah H, Zarnani A, et al. Comparative immunophenotypic characteristics, proliferative features, and osteogenic differentiation of stem cells isolated from human permanent and deciduous teeth with bone marrow. Mol Biotechnol. 2016;58(6):415–27.
35. Jamie M, Chrisna D, Michael SP. An in vitro and in vivo comparison of osteogenic differentiation of human mesenchymal stromal/stem cells. Stem Cells Int. 2021;2021:0.
36. Labedz-Maslowska A, Bryniarska N, Kubiak A, Kaczmarzyk T, Sekula-Stryjewska M, Noga S et al. Multilineage differentiation potential of human dental pulp stem cells-impact of 3D and hypoxic environment on osteogenesis in vitro. Int J Mol Sci. 2020;21(17).
37. Sheyn D, Shapiro G, Tawackoli W, Jun DS, Koh Y, Kang KB, et al. PTH induces systemically administered mesenchymal stem cells to migrate to and regenerate spine injuries. Mol Ther. 2016;24(2):318–30.
38. Wang J, Li J, Yang L, Zhou Y, Wang Y. Dose-dependence of PTH-related peptide-1 on the osteogenic induction of MC3T3-E1 cells in vitro. Medicine. 2017;96(17).
39. Korpelainen R, Keinänen-Kiukaanniemi S, Heikkinen J, Väänänen K, Korpelainen J. Effect of exercise on extraskeletal risk factors for hip fractures in elderly women with low BMD: a population-based randomized controlled trial. J Bone Mineral Research: Official J Am Soc Bone Mineral Res. 2006;21(5):772–9.
40. J R Z. RMNCDA. Effect of parathyroid hormone (1–34) on fractures and bone mineral density in postmenopausal women with osteoporosis. N Engl J Med. 2001;344:19.
41. Tanja S, Lars R, Jesper Skovhus T, Anna T, Annemarie B, Gratien A et al. Changes in 3-dimensional bone structure indices in hypoparathyroid patients treated with PTH(1–84): a randomized controlled study. J Bone Min Res. 2011;27(4).
42. Juan GG-Q, Juan YDR, Carlos AMV, Sofía PA, M V.-G. J C M., S. Critical-sized mandibular defect reconstruction using human dental pulp stem cells in a xenograft model-clinical, radiological, and histological evaluation. Oral Maxillofacial Surg. 2020;24(4).
43. Lyu J, Hashimoto Y, Honda Y, Matsumoto N. Comparison of osteogenic potentials of dental pulp and bone marrow mesenchymal stem cells using the new cell transplantation platform, cellSaic, in a rat congenital cleft-jaw model. Int J Mol Sci. 2021;22(17):9478.
44. Alge DL, Zhou D, Adams LL, Wyss BK, Shadday MD, Woods EJ, et al. Donor-matched comparison of dental pulp stem cells and bone marrow-derived mesenchymal stem cells in a rat model. J Tissue Eng Regen Med. 2010;4(1):73–81.
45. Alarcón-Apablaza J, Prieto R, Rojas M, Fuentes R. Potential of oral cavity stem cells for bone regeneration: A scoping review. Cells. 2023;12(10).
46. Xingyun G, Zehan L, Shuanglin J, Yanqiu W, Na L, Jiamin L et al. Parathyroid hormone enhances the osteo/odontogenic differentiation of dental pulp stem cells via ERK and P38 MAPK pathways. J Cell Physiol. 2019;235(2).
47. Mi-Ra K, Sung-Hyeon C, Bin-Na L, Kyung-San M, Yun-Chan H. Effect of parathyroid hormone-related protein on odontogenic differentiation in human dental pulp cells. BMC Oral Health. 2020;20(1).
48. Liu QH, Liao LM, Wu H, Lin YP, Yu S. PTH promotes rabbit tibial fracture healing via the Notch signaling pathway. Eur Rev Med Pharmacol Sci. 2020;24(4):1616–23.
49. Mousaei Ghasroldasht M, Seok J, Park HS, Liakath Ali FB, Al-Hendy A. Stem cell therapy: from Idea to clinical practice. Int J Mol Sci. 2022;23(5).
50. Chen T, Wang Y, Hao Z, Hu Y, Li J. Parathyroid hormone and its related peptides in bone metabolism. Biochem Pharmacol. 2021;192:114669.
51. Xu M, Li Y, Feng X, Zheng W, Zhao Z, Li Y. Parathyroid hormone promotes maxillary expansion and reduces relapse in the repeated activation maxillary expansion rat model by regulating Wnt/β-catenin pathway. Prog Orthodont. 2022;23(1):1.
52. Liu D, He S, Chen S, Yang L, Yang J, Bao Q, et al. Different effects of Wnt/β-catenin activation and parathyroid hormone on diaphyseal and metaphyseal in the early phase of femur bone healing of mice. Clin Exp Pharmacol Physiol. 2019;46(7):652–63.
53. Xie Z, Yan D, Zhou Q, Wu Z, Weng S, Boodhun V, et al. The fast degradation of β-TCP ceramics facilitates healing of bone defects by the combination of BMP-2 and teriparatide. Volume 112. Biomedicine & pharmacotherapy = Biomedecine & pharmacotherapie; 2019. p. 108578.
54. Kanezaki S, Miyazaki M, Ishihara T, Notani N, Abe T, Tsubouchi Y, et al. Enhancement of the effects of intermittent parathyroid hormone (1–34) by bone morphogenetic protein in a rat femoral open fracture model. J Orthop Surg Res. 2019;14(1):403.
55. Wang G, Yuan N, Li N, Wei Q, Qian Y, Zhang J, et al. Vascular endothelial growth factor mimetic peptide and parathyroid hormone (1–34) delivered via a blue-light-curable hydrogel synergistically accelerate bone regeneration. ACS Appl Mater Interfaces. 2022;14(31):35319–32.

Publisher's note